ELSEVIER

Catalysis Today 33 (1997) 161–171

CATALYSIS TODAY

Improved method of preparation of vanadium phosphate catalysts

Graham J. Hutchings [a,*], Maria T. Sananes [b], Sujata Sajip [c], Christopher J. Kiely [a,c], Andy Burrows [c], Ian J. Ellison [a], Jean Claude Volta [b]

[a] *Leverhulme Centre for Innovative Catalysis, Department of Chemistry, University of Liverpool, PO Box 147, Liverpool, L69 3BX, UK*
[b] *Institut de Recherches sur la Catalyse, CNRS, 2 Avenue Albert Einstein, 69626, Villeurbanne Cedex, France*
[c] *Department of Materials Science and Engineering, University of Liverpool, P.O. Box 147, Liverpool, L69 3BX, UK*

Abstract

The preparation of vanadium phosphorus oxide catalysts for the oxidation on n butane to maleic anhydride is discussed. In particular the preparation route based on the reduction of $VOPO_4 \cdot 2H_2O$ with alcohols is described in detail and contrasted with two other preparation methods: (i) using aqueous HCl as a reductant for V_2O_5 and (ii) using isobutanol as reductant and solvent for V_2O_5. The catalytic performance of final catalysts prepared by in situ transformation under the reaction conditions is contrasted. It is found that catalysts derived from the reduction of $VOPO_4 \cdot 2H_2O$ with 1-alcohols tend to give high activity catalysts by virtue of the high surface area material (typically 40 $m^2\ g^{-1}$) generated by this synthetic method. The preparation of $VO(H_2PO_4)_2$ by two routes is also described and it is shown that when this material is used as a catalyst precursor, final catalysts are ultra-selective for formation of maleic anhydride, together with furan. The characterisation of all these catalysts using various electron microscopy techniques is described and the morphology of the active catalysts is discussed.

Keywords: Vanadium phosphate catalysts; n-Butane oxidation; Maleic anhydride; Transmission electron microscopy; High resolution electron microscopy

1. Introduction

Vanadium phosphorus oxide catalysts represent the only example of a commercial catalyst for the selective oxidation of an alkane, namely n butane to maleic anhydride. In view of this, the catalyst has been extensively studied [1,2] and it has been recently shown that this catalyst can also be effective for other partial oxidation reactions, including the ammoxidation of propane [3,4] and the oxidation of pentane to phthalic anhydride [5,6]. Vanadium phosphorus catalysts were first noted as being effective for butane oxidation to maleic anhydride in 1966 [7]. Since then a variety of well defined compounds have been prepared and characterised, e.g., $VOHPO_4 \cdot 0.5H_2O$, α_I-, α_{II}-, β-, γ-, δ-$VOPO_4$, $VOPO_4 \cdot 2H_2O$, $(VO)_2P_2O_7$, $VO(H_2PO_4)_2$, $VO(PO_3)_2$ [8]. To date most work has been concentrated on the preparation of catalysts using $VOHPO_4 \cdot 0.5H_2O$ as the catalyst precursor, which under certain reaction conditions has been shown to topotactically transform to give mainly $(VO)_2P_2O_7$ [9]. One of the main features of vanadium phosphorus oxide catalystsis that although the bulk composition of active catalysts has a V:P ratio of 1:1, the surface is considerably enriched with phospho-

* Corresponding author.

PII S0920-5861(96)00111-3

rus. Most workers agree that surface P:V ratios > 1.5 are typically observed [8]. The role of excess surface phosphorus is as yet unclear, but it is known that these catalysts deactivate by phosphorus loss and it is possible that the excess surface phosphorus could play a role in controlling the oxidation state of the surface vanadium atoms or could act to provide site isolation.

As the transformation is topotactic, it follows that the morphology of the catalyst precursor will control the morphology of the final catalyst. Hence, careful control of the precursor preparation procedure is of immense importance. A number of preparation routes for the hemihydrate precursor $VOHPO_4 \cdot 0.5H_2O$ have been investigated. Early methods were based on the use of HCl as reducing agent with either aqueous or alcohol solvents [10]. Johnson et al. [9] described a method based on the reduction of $VOOHPO_4 \cdot 0.5H_2O$ using C_2–C_4 alcohol's and these results were confirmed by Horowitz et al. [11]. However, in these earlier studies, alcohols with higher C number than C_4 were not investigated. We have investigated a wide range of alcohols as reducing agents and have found that by careful selection of the alcohol, either (i) high area catalysts based on $VOHPO_4 \cdot 0.5H_2O$ as precursor can be prepared or (ii) ultraselective catalysts based on $VO(H_2PO_4)_2$ as precursor can be synthesised [12]. In this paper we describe and discuss the performance of these catalysts and provide a detailed structural characterisation of the materials using electron microscopy.

2. Experimental

2.1. Catalyst preparation based on $VOPO_4 \cdot 2H_2O$

$VOPO_4 \cdot 2H_2O$ was prepared by reacting V_2O_5 (5.0 g) with H_3PO_4 (30 ml, 85%) in water (120 ml) under reflux for 24 h. The yellow solid was recovered by filtration, washed sparingly with water, followed by acetone and dried (air, 110°C). VOPO4 $\cdot 2H_2O$ was then refluxed with predried alcohols for 20 h (50 mol alcohol/mol $VOPO_4 \cdot 2H_2O$) and the solid product was recovered by filtration and dried (air, 110°C, 16 h).

Catalysts based on the aqueous HCl and standard alcohol routes were prepared for comparison as previously described [13].

2.2. Catalyst testing

The oxidation of n-butane was carried out using a microreactor working under differential conditions using a known volume of catalyst (0.6–0.7 ml). A feedstock composition of butane/oxygen/helium = 1.5/18.5/80 and a total feed gas flow rate of 1000 ml gas/ml catalyst/h were employed. Reactants and products were analysed by on-line gas chromatography and satisfactory mass balances were obtained for all data presented (98–100%). The following catalyst testing procedure was adopted irrespective of the precursor preparation procedure. The precursor was loaded to the reactor and the flow of the feed gases was established; following this, the precursor was heated to the reaction temperature of 370°C at a rate of 3°C min^{-1}. During this treatment the catalyst precursor was transformed in situ in the reactor and the catalyst performance gradually improved. The catalyst was allowed to stabilise for 72 h.

2.3. Catalyst characterisation

The catalyst precursors were characterised by powder X-ray diffraction and scanning electron microscopy. The final catalysts were characterised by transmission electron microscopy in addition to powder X-ray diffraction and scanning and transmission electron microscopy.

An Hitachi S-2460-N scanning electron microscope was used to obtain topographical information on both the precursors and the final catalysts. Samples suitable for transmission electron microscopy (TEM) were prepared by

dispersing the catalyst powder onto a lacey carbon film supported on a copper mesh grid. TEM observations were made in a JEOL 2000EX high resolution electron microscope operating at 200 kV. This instrument was fitted with a low light level TV camera and frame averaging system to allow us to use very low illumination conditions. This latter condition is essential for the study of beam sensitive vanadium phosphorus oxide catalysts. Images were recorded on S-VHS videotape, individual frames for which could be subsequently captured into a Macintosh Quadra computer for enhancement and detailed analysis.

3. Results

3.1. Preparation of VPO catalysts from $VOPO_4 \cdot 2H_2O$

The reduction of $VOPO_4 \cdot 2H_2O$ was studied using a wide range of alcohols. Initially, a series of primary and secondary alcohols were studied and the products were characterised using pow-

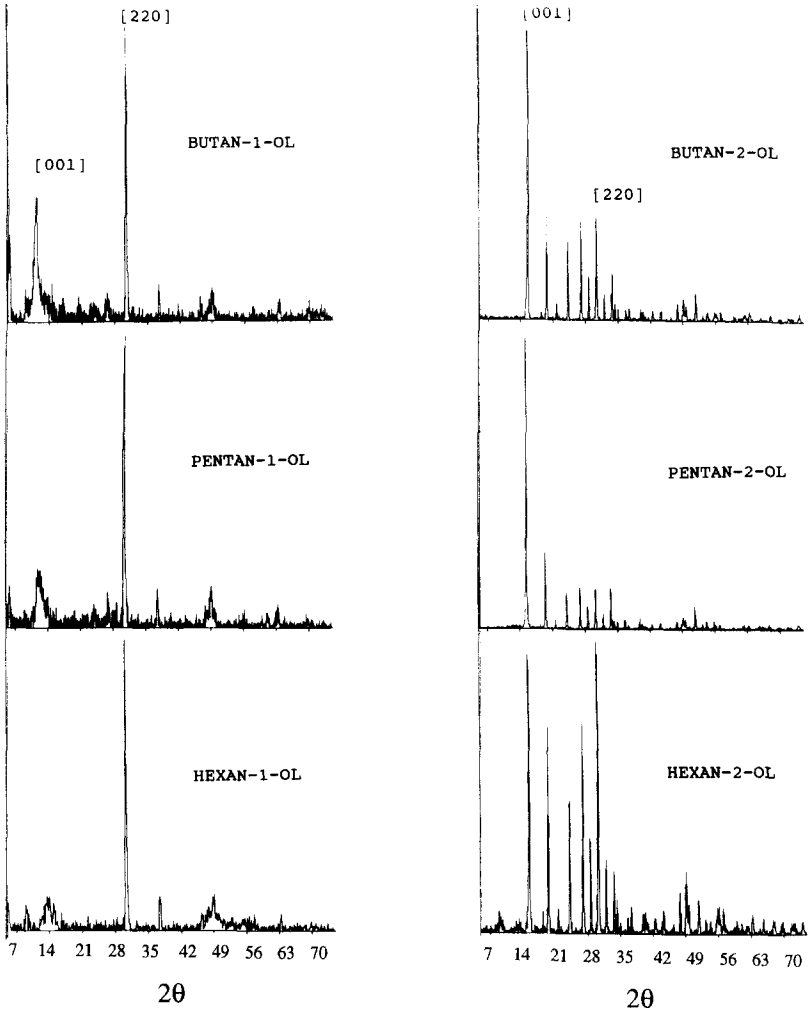

Fig. 1. Powder X-ray diffraction patterns of the precursor prepared primary and secondary alcohols.

der X-ray diffraction and typical results for primary and secondary alcohols are given in Fig. 1. It is apparent that use of a primary alcohol as the reducing agent leads to the formation of $VOHPO_4 \cdot 0.5H_2O$ crystals for which the [220] reflection is virtually the only feature of the diffraction pattern. In contrast, secondary alcohols lead to the formation of $VOPO_4 \cdot 0.5H_2O$ for which the [001] reflection is the dominant feature of the diffraction pattern, but it is clear that many other diffraction lines are also present and the diffraction pattern is similar to that observed for $VOHPO_4 \cdot 0.5H_2O$ prepared by a variety of methods [8,9]. These results indicate that the $VOHPO_4 \cdot 0.5H_2O$ prepared using primary and secondary alcohols exhibit distinctly different morphologies, which has been confirmed by scanning electron microscopy of the materials prepared using 1-, 2- and 3-hexanol (Fig. 2). The precursor prepared from 1-hexanol is made up of thin platelets (ca. 1 μm in diameter and 60 nm in thickness) densely packed to form 'rose-like' cluster, and this is typical for $VOHPO_4 \cdot 0.5H_2O$ prepared using a primary alcohol. The surface areas of $VOHPO_4 \cdot 0.5H_2O$ prepared by using primary alcohols was typically in the range 30–45 $m^2 g^{-1}$ and therefore represents a preparative route

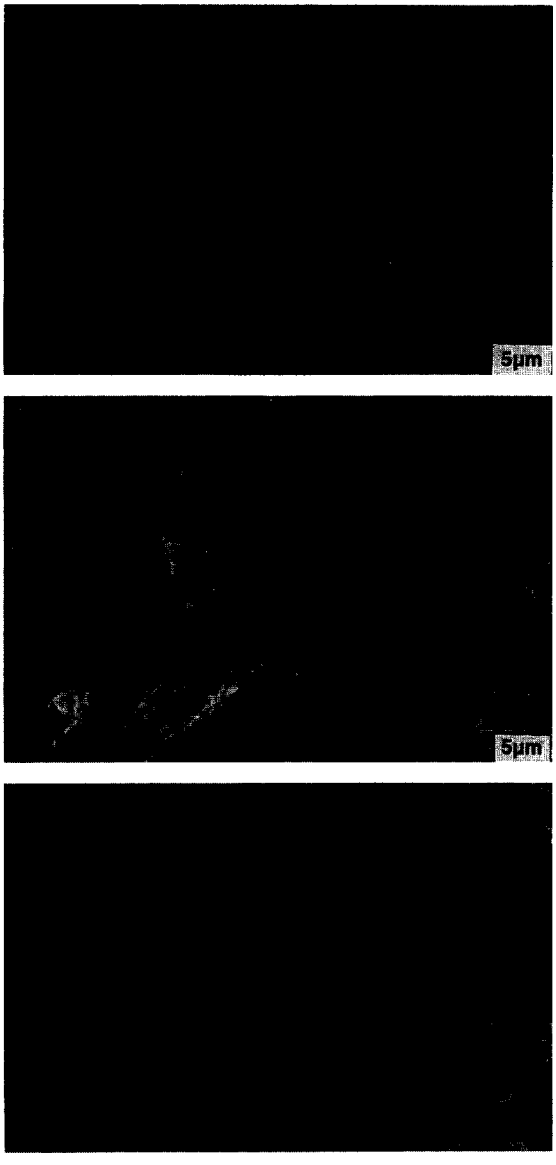

Fig. 2. SEM micrographs of the precursors prepared from (a) 1-hexanol, (b) 2-hexanol and (c) 3-hexanol.

Table 1
Product types derived from the reaction of $VOPO_4 \cdot 2H_2O$ with various alcohols [12] [a]

Alcohol	Product type [b]
2-Methyl-1-propanol	1
Butanol	1
2-Butanol	2
Butenol	2
1-Pentanol	1
2-Pentanol	2
3-Pentanol	2
1-Hexanol	1
2-Hexanol	2
3-Hexanol	2
1-Heptanol	1
2-Heptanol	2
3-Heptanol	2
1-Octanol	1
2-Octanol	2
3-Octanol	3
1-Nonanol	1
2-Nonanol	2
3-Nonanol	2
1-Decanol	1
2-Decanol	2
3-Decanol	2

[a] Reaction under reflux, 20 h.
[b] Type 1 as Fig. 1a (high surface area rosette structures).
Type 2 as Fig. 1b (lower surface area hemihydrate platelets).
Type 3 $VO(H_2PO_4)_2$.

to a high area catalyst. The precursors prepared using secondary alcohols typically consist of discrete randomly orientated platelets whose lateral dimensions are typically 2–4 μm and thicknesses are typically 200 nm (Fig. 2b and Fig. 2c). The surface areas of $VOHPO_4 \cdot 0.5H_2O$ prepared using secondary alcohols were much lower, typically in the range 5–10 $m^2\ g^{-1}$.

Subsequently, a wide range of C_4–C_{12} alcohols were investigated for the reduction of $VOPO_4 \cdot 2H_2O$ and the results of these studies are given in Table 1. It is apparent that the use of most alcohols give $VOHPO_4 \cdot 0.5H_2O$ as the product. However, 3-octanol as reducing agent leads to exclusive formation of $VO(H_2PO_4)_2$ and in this special case $VOHPO_4 \cdot 0.5H_2O$ was only observed as a minor impurity in some preparations. Previously, $VO(H_2PO_4)_2$ has been prepared in pure form via V_2O_4 [14] however, this new method based on the reaction of $VOPO_4 \cdot 2H_2O$ with 3-octanol represents a novel and simple preparative route to this material.

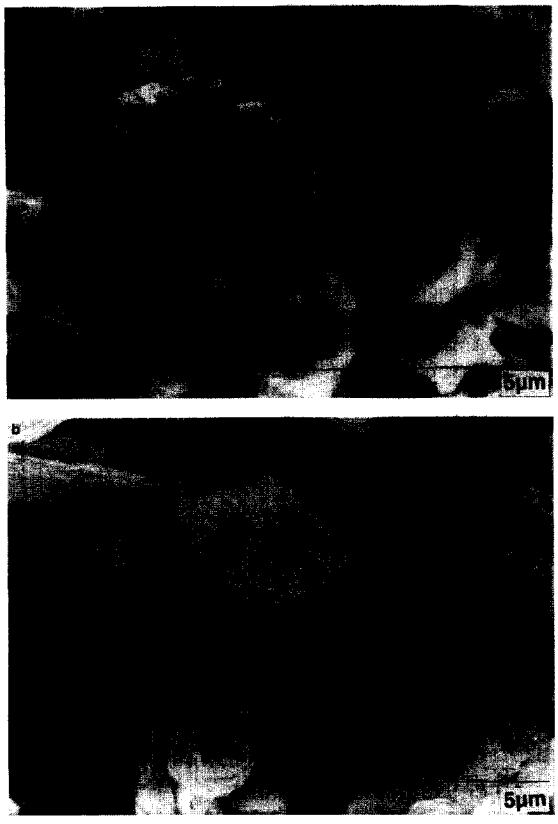

Fig. 3. SEM micrographs of (a) precursor prepared by reaction of $VOPO_4 \cdot 2H_2O$ with isobutanol and (b) the final activated catalyst.

3.2. Comparison of $VOPO_4 \cdot 2H_2O$ derived catalysts with aqueous HCl and isobutanol preparation

The catalytic performance of a catalyst prepared from the precursor derived from the reduction of $VOPO_4 \cdot 2H_2O$ with a primary alcohol (isobutanol) has been compared with catalysts derived from two other $VOHPO_4 \cdot 0.5H_2O$ precursors prepared either (I) using aqueous HCl as a reducing agent for V_2O_5 [15] or (ii) using isobutanol as solvent and reducing agent for V_2O_5 [15]. The catalytic data obtained after 72 h time on line are given in Table 2 and at this stage the catalytic performance of all the

Table 2
Comparison of the catalytic performance of final catalysts derived from $VOHPO_4 \cdot 0.5H_2O$ prepared via different routes

Catalyst	$S_{BET}/m^2\ g^{-1}$		n-Butane [a] conv./%	Product selectivity/%		
	Precursor	Final catalyst		MA	CO	CO_2
VPA [b]	3	4	11	51	41	7
VPO [c]	11	14	27	52	34	14
VPD [d]	32	43	62	64	21	14

[a] Reaction condition: 72 h activation, 385°C, 1.5% n-butane in air; GHSV = 1000 h^{-1}.
[b] VPA = catalyst precursor prepared by reduction of V_2O_5 with aqueous HCl.
[c] VPO = catalyst precursor prepared by reduction of V_2O_5 with isobutanol.
[d] VPD = catalyst precursor prepared by refluxing $VOPO_4 \cdot 2H_2O$ with isobutanol.

Table 3
Catalytic performance of catalysts prepared from $VO(H_2PO_4)_2$ [a]

Catalyst precursor	T/°C	Conv./%	Product selectivity (%) [b]			Specific activity (mol MA m^{-2} h^{-1})
			MA	F	CO_x	
$VO(H_2PO_4)_2$ ex 3-octanol [c]	375	4	100	0	0	2.36×10^{-5}
$VO(H_2PO_4)_2$ ex V_2O_4 [d]	375	5	67	33	0	1.73×10^{-5}
VPA [e]	385	11	51	0	48	1.24×10^{-5}
VPO [f]	385	27	52	0	48	1.35×10^{-5}

[a] Reaction conditions: GHSV = 1000 h^{-1}, 1.5% butane in air, 24 h.
[b] MA = maleic anhydride F = furan.
[c] Surface area of final catalyst 2.2 m^2 g^{-1}.
[d] Surface area of final catalyst 1 m^2 g^{-1}
[e] VPA = catalyst precursor prepared by reduction of V_2O_5 with aqueous HCl.
[f] VPO = catalyst precursor prepared by reduction of V_2O_5 with isobutanol.

materials had stabilised. It is clear that the material derived from $VOPO_4 \cdot 2H_2O$ is considerably more active and selective to maleic anhydride when compared with the other catalysts. However, this difference in activity is largely due to the enhanced surface area of this catalyst, which results from the high surface area of the precursor being retained on activation, and all three catalysts display virtually the same specific activity of ca. 1.2×10^{-5} mol MA m^{-2} h^{-1}. It is therefore apparent that the distribution of active sites is similar for these catalysts. The advantage gained by using the preparative route based on the reduction of $VOPO_4 \cdot 2H_2O$ with a primary alcohol, is that it provides a simple and reliable method for the preparation of a high area catalyst.

3.3. Catalytic performance of materials derived from the $VO(H_2PO_4)_2$ precursor

As noted previously, reduction of $VOPO_4 \cdot 2H_2O$ with 3-octanol leads to the formation of $VO(H_2PO_4)_2$ and not $VOHPO_4 \cdot 0.5H_2O$, which is observed with all other alcohols tested to date. Two samples of $VO(H_2PO_4)_2$ were prepared, one using the new 3-octanol route and the other from V_2O_4 as described by Bordes

Fig. 4. TEM micrograph of final catalyst prepared using isobutanol as solvent and reducing agent.

[14]. These two samples were then transformed in situ in the microreactor under the standard activation conditions (400°C, 1.5% n-butane in air) and the performance was allowed to stabilise for 72 h. The resultant catalytic data are given in Table 3, and for comparison the results for catalysts prepared via the $VOHPO_4 \cdot 0.5H_2O$ precursor from the aqueous HCl reduction of V_2O_5 and the isobutanol reduction of V_2O_5 are also shown. It is apparent that the $VO(H_2PO_4)_2$ derived catalysts display ultraselective formation of maleic anhydride and no carbon oxides are observed. In contrast the catalytic performance of the $VOHPO_4 \cdot 0.5H_2O$ derived catalysts show the formation of carbon oxides typically expected under this condition. It is also interesting to note that $VO(H_2PO_4)_2$ prepared from V_2O_4 also gives some selectivity to furan. This is extremely unusual since under these reaction conditions, furan is not observed as a product with $VOHPO_4 \cdot 0.5H_2O$ derived catalysts.

3.4. Characterisation of $VOPO_4 \cdot 2H_2O$ derived catalysts using electron microscopy

3.4.1. Catalysts prepared by reaction of $VOPO_4 \cdot 2H_2O$ with isobutanol

Fig. 3 shows an SEM micrograph of both the catalyst precursor $VOHPO_4 \cdot 0.5H_2O$ and the final catalyst of the material prepared by the reaction of $VOPO_4 \cdot 2H_2O$ with isobutanol. The precursor is made up of platelets (ca. 1 μm in diameter and 0.1 μm in thickness) arranged in the characteristic 'rose-like' clusters, as was observed for the material prepared from 1-hexanol (Fig. 2a). The SEM micrograph of the final catalyst demonstrates that a topotactic transformation has occurred in this case, since the activated material has retained distinctive morphology of the precursor.

The final catalyst does, however, also show isolated platelet crystallites with lateral dimensions of about 1 μm. The X-ray diffraction pattern for this material can be indexed to the $(VO)_2P_2O_7$ structure, and the ^{31}P spin echo mapping NMR spectrum [15] is characteristic of $(VO)_2P_2O_7$ (signal at 2600 ppm) with a small amount of $VOPO_4$ type phases (signal at 0 ppm). TEM examination of the final catalyst shows a combination of large isolated platelets and rosette shaped clusters as shown in Fig. 4. The rosette-type agglomerates, which are the majority phase and constitute ca. 95 vol%, have been studied by HREM (see Fig. 5a). Analysis of the fringe spacings and the intersection an-

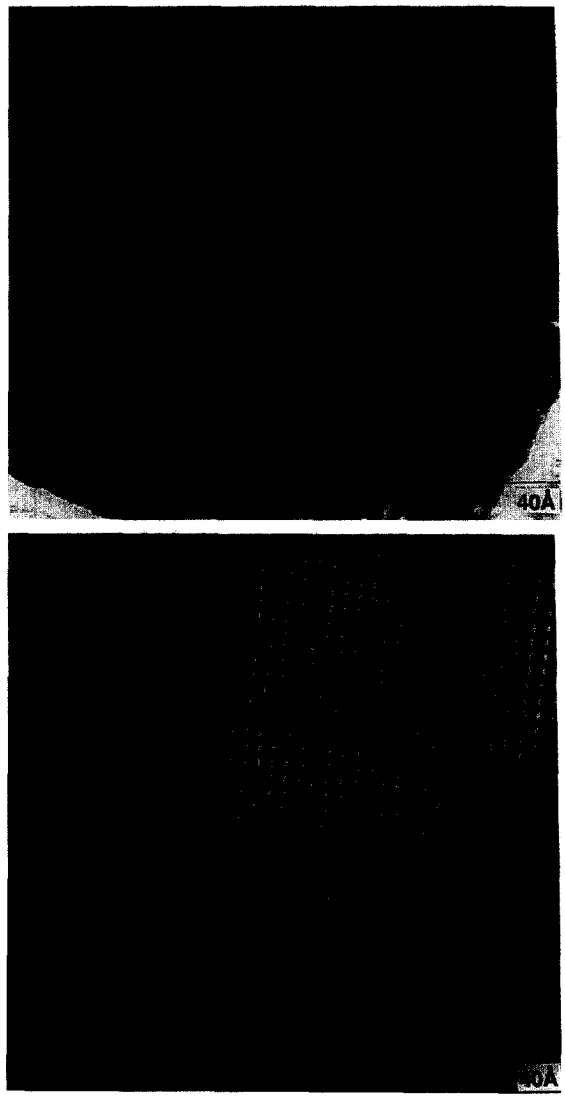

Fig. 5. (a) An axial [100] HREM lattice image from an individual $(VO)_2P_2O_7$ platelet in the rosette structure. (b) an axial [001] HREM image from an isolated α_{II}-$VOPO_4$ platelet.

gles from this image which was obtained normal to a platelet in the rosette, confirm that the image is the [100] projection of $(VO)_2P_2O_7$. Hence, the rosette type structures are made up of agglomerates of $(VO)_2P_2O_7$ and these are typically less than 400 nm in size. The large isolated platelets were found by a combination of selected area diffraction analysis and HREM to be α_{II}-$VOPO_4$ and these account for about 3–4 vol% of the sample. Fig. 5b shows an axial [001] HREM image of α_{II}-$VOPO_4$ in which the 200 and 020 lattice spacings (both ~0.3 nm) are resolved. A third morphology (Fig. 6a) has been observed in the activated catalysts. These platelets, which are typically 0.1–0.2 μm in size, are much more beam sensitive and struc-

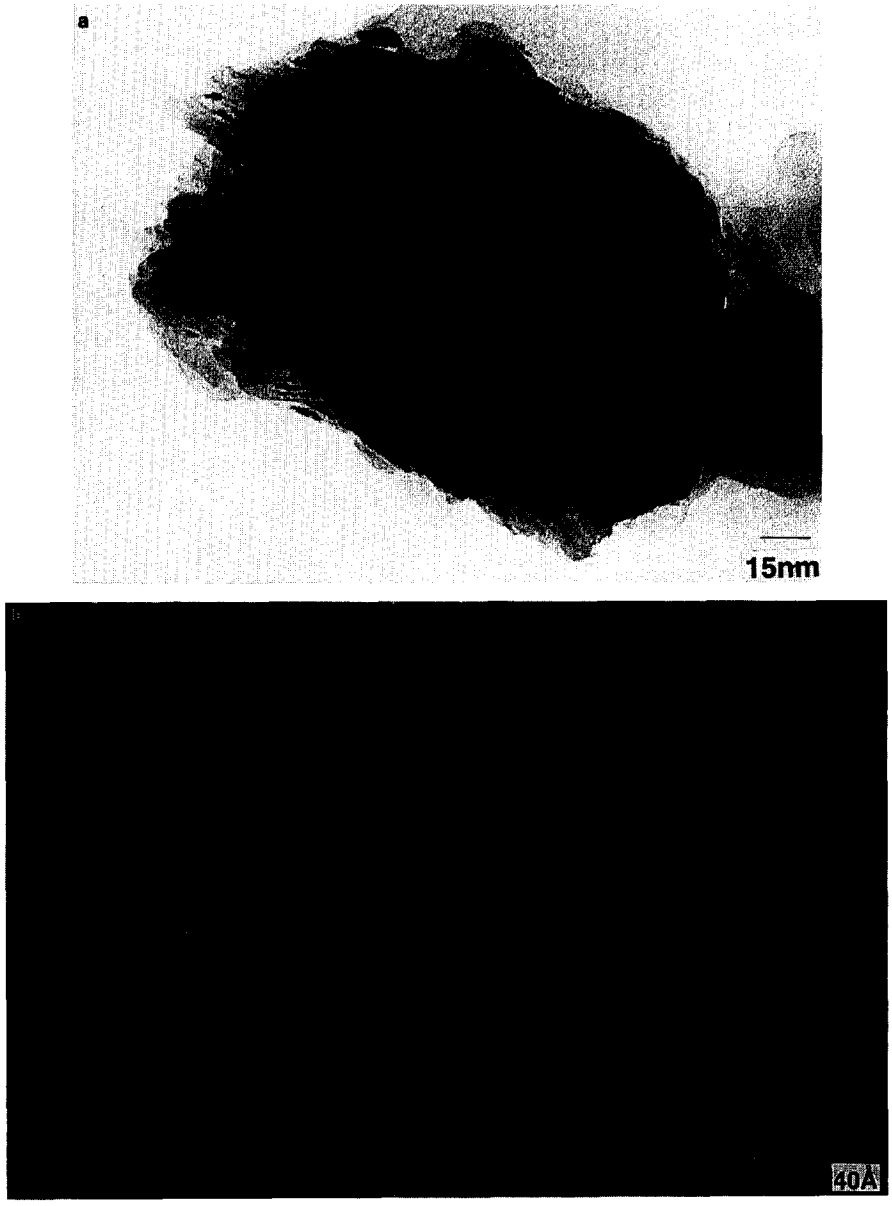

Fig. 6. (a) A disordered $(VO)_2P_2O_7$ grain showing crystalline surface patches. (b) The lattice image from a crystalline patch corresponding to the [021] projection of $(VO)_2P_2O_7$.

Fig. 7. Bright field micrographs showing fragments of $(VO)_2P_2O_7$ supported on α_{II}-$VOPO_4$.

turally disordered than $(VO)_2P_2O_7$ or α_{II}-$VOPO_4$. A clear feature of this morphology type is that elongated raft-like patches (typically 15×5 nm) of a second phase were always observed on the surface of these platelets. When observed by HREM (Fig. 6b) the surface patches were always found to be more under the electron beam than the underlying platelet. The HREM of the surface patch (Fig. 6b) shows a 0.3 nm (d_{200}) set of fringes that run parallel to the long axis and a 0.32 nm (d_{024}) set of fringes in the perpendicular direction. These correspond to the [021] projection of $(VO)_2P_2O_7$ and hence we have tentatively assigned the third morphology as being the remnants of a hemihydrate precursor crystallite which has only partially transformed to $(VO)_2P_2O_7$. In addition, occasionally crystallites of $(VO)_2P_2O_7$ are observed to be supported on α_{II}-$VOPO_4$ in random orientations as shown in Fig. 7.

3.4.2. *Catalysts prepared by reaction of $VOPO_4 \cdot 2H_2O$ with 3-octanol*

Fig. 8 shows an SEM micrograph of both the catalyst precursor $VO(H_2PO_4)_2$ prepared by the reaction of $VOPO_4 \cdot 2H_2O$ with 3-octanol and final activated catalyst. The precursor shows a 'block-like' morphology which is retained in the final catalyst with one rather subtle difference being apparent. In the final catalyst, the rectangular surfaces of the oblong crystals show regular corrugations in the surface with a periodicity of about 200 nm, whereas the end phases

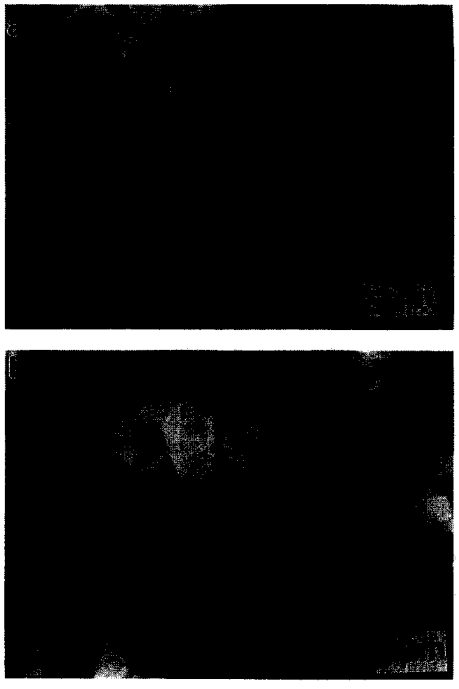

Fig. 8. SEM micrograph of the final catalyst prepared from $VO(H_2PO_4)_2$ ex 3-octanol.

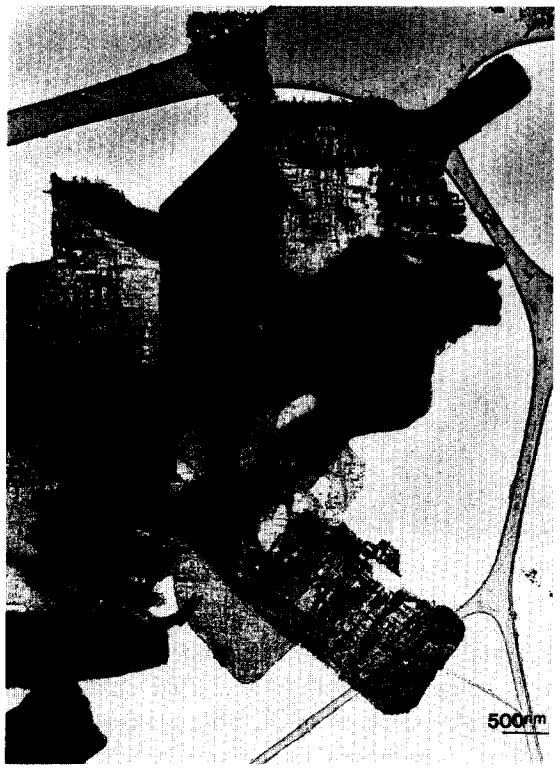

Fig. 9. Bright field TEM micrograph of the final catalyst prepared from 3-octanol.

remain smooth. It is possible that these are caused by dehydration of the precursor during transformation to the final catalyst. The X-ray diffraction pattern obtained from the final catalyst is highly disordered, but there are some reflections that are characteristic of $VO(PO_3)_2$ and $VO(H_2PO_4)_2$. Fig. 9 shows a bright field TEM micrograph of this $VO(PO_3)_2$ sample in which the corrugations on the surface of the blocky crystallite are evident.

4. Discussion

It is clear from the preceding results that using $VOPO_4 \cdot 2H_2O$ as a starting point for the preparation of vanadium phosphorus catalysts leads to the synthesis of two interesting types of materials: (a) it provides a method for producing a high surface area form of $VOHPO_4 \cdot 0.5H_2O$ that can be topotactically transformed to a high surface area (30–40 $m^2\ g^{-1}$) final catalyst comprising mainly $(VO)_2P_2O_7$; (b) it also provides a new route to the synthesis of $VO(H_2PO_4)_2$ which in turn has been found to provide ultra-selective catalysts for the synthesis of maleic anhydride.

Previous routes for the synthesis of high area precursors have been based on ball milling or mechanical grinding of the catalyst precursor [16]. Hence the use of primary alcohols to reduce and dehydrate $VOPO_4 \cdot 2H_2O$ to $VOHPO_4 \cdot 0.5H_2O$ provides a novel procedure for the reliable synthesis of high area materials that negates the need for any mechanical grinding of the precursor.

We have found that the final catalyst prepared from the precursor formed by the reaction of $VOPO_4 \cdot 2H_2O$ with isobutanol contains a mixture of $(VO)_2P_2O_7$ (95 vol%), α_{II}-$VOPO_4$ (3–4 vol%) and possibly some partially-transformed hemihydrate (1–2 vol%). The observation of this partially transformed material indicates that the in situ activation procedure had not been completed, even though it has been carried out for 72 h. It is known that formation of the equilibrated catalysts can take many days, and so it is perhaps not unreasonable that partially transformed material is still present at this stage. Having noted that the catalytic performance of the catalyst had stabilised well before 72 h it is apparent that the minor amount of non-transformed material was not detrimental to the catalyst performance. Previous TEM and HREM studies of the $VOHPO_4 \cdot 0.5H_2O$ precursor prepared by aqueous HCl reduction of V_2O_5 or by isobutanol reduction of V_2O_5 [15] have also shown that the final catalyst comprise mainly $(VO)_2P_2O_7$ and α_{II}-$VOPO_4$. Despite the fact that all three final catalysts display very different volume fractions of $(VO)_2P_2O_7$ and α_{II}-$VOPO_4$, but the specific activity of the final catalyst are very similar (ca. 1.2×10^{-5} mol MA $m^2\ h^{-1}$). Such a result suggests that alternative explanations, either (i) the phases present are all equally active, or (ii) only a small proportion of the surface is active and this small

proportion is equally exposed in all the catalyst types. The second explanation seems most likely, since it is known that by itself α_{II}-$VOPO_4$ is non-selective, and two possibilities exist in this case. First, it is possible that a contact synergy exists between the separate α_{II}-$VOPO_4$ and $(VO)_2P_2O_7$ phases and these contacts are known to be present as shown in Fig. 7. Second, the active sites are present at surface defects as suggested by a recent HREM study [17]. It is clear that considerable further work is necessary to address this fascinating question.

The synthesis of final catalysts capable of ultraselective synthesis of maleic anhydride when $VO(H_2PO_4)_2$ is used as a precursor is also of great interest. One possibility, of course, is that the maleic anhydride merely results from impurities of $VOHPO_4 \cdot 0.5H_2O$ remaining in the catalyst precursor that transform to a well dispersed low volume fraction of $(VO)_2P_2O_7$. There are a number of factors that mitigate against this explanation. First, the $VO(H_2PO_4)_2$ precursor is purified by water extraction and recrystallisation. Second, the specific activity of the final catalyst is considerably higher than catalysts typically prepared from $VOHPO_4 \cdot 0.5H_2O$. Third, the primary selectivity of catalysts prepared from $VOHPO_4 \cdot 0.5H_2O$ is typically 85–90% and in this case selectivities of 100% are observed. Based on this analysis, it is apparent that a new high activity and high selectivity active site has been created in the surface of the catalyst. It is worth noting that X-ray photoelectron spectroscopy of $VO(H_2PO_4)_2$ derived catalysts [18] indicates that the surface P/V ratio of these catalysts is ca. 4.0. This is considerably higher than the P/V of ca. 2.0 surface ratio usually observed with $VOHPO_4 \cdot 0.5H_2O$ derived catalysts. It is possible that the higher surface P concentration may contribute to the creation of the high activity site possibly via a site isolation mechanism and further studies on this aspect are now in progress.

Acknowledgements

We thank the EC HCM fund (contract CHRX-CT92-0065) and the EPSRC for financial support.

References

[1] G. Centi, F. Trifiro, J.R. Ebner and V.M. Franchetti, Chem. Rev. 88 (1988) 55.
[2] G.J. Hutchings, Appl. Catal. 72 (1991) 1.
[3] G. Centi, T. Tosarelli and F. Trifiro, J. Catal. 142 (1993) 70.
[4] G. Centi and S. Perathoner, J. Catal. 142 (1993) 84.
[5] G. Centi and F. Trifiro, Catal. Sci. Technol. 1 (1991) 225.
[6] F. Trifiro, Catal. Today 16 (1993) 91.
[7] R.L. Bergmann and N.W. Frisch, US Pat. 3293268, 1966 to Princeton Chemical Research.
[8] G. Centi ed., Catal. Today 16 (1) (1993).
[9] J.W. Johnson, D.C. Johnson, A.J. Johnson and J.F. Brady, J. Am. Chem. Soc. 106 (1984) 8123.
[10] J.P. Harrison, US Pat. 3985775, 1976, to Chevron Research Co; R.A. Sneider, US Pat. 3864280, 1975; US Pat. 4043943, 1977 to Chevron Research Co.
[11] H.S. Horowitz, C.M. Blackstone, A.W. Sleight and G. Truffer, Appl. Catal. 38 (1988) 193.
[12] I.J. Ellison, G.J. Hutchings, M.T. Sananes and J.C. Volta, J. Chem. Soc., Chem. Commun. (1994) 1093; M.T. Sananes, G.J. Hutchings and J.C. Volta, J. Chem. Soc., Chem. Commun. (1995) 243.
[13] G.J. Hutchings and R. Higgins, UK Pat. 1601121, 1981, to ICI.
[14] E. Bordes, Catal. Today 1 (1987) 499.
[15] C.J. Kiely, A. Burrows, S. Sajip, G.J. Hutchings, M.S. Sananes, A. Tuel and J.C. Volta, J. Catal. in press.
[16] G.J. Hutchings and R. Higgins, US Pat. 4317717, to ICI.
[17] P.L. Gai and K. Kourtakis, Science 267 (1995) 661.
[18] M.T. Sananes, G.J. Hutchings and J.C. Volta, J. Catal. 154 (1995) 253.